ARCHIVES OF ELECTRICAL ENGINEERING VOL. 71(4), pp. 895–907 (2022)

DOI 10.24425/aee.2022.142115

Virtual synchronous generator frequency response study of energy computing and storage devices

Baoge Zhang, Shanyan Ping ✉, Yi Long, Yuemin Jiao, Boxiang Wu

School of Automation and Electrical Engineering, Lanzhou Jiaotong University
China

e-mail: bgzhang@mail.lzjtu.cn, ✉pingshanyan@foxmail.com

(Received: 18.03.2022, revised: 12.07.2022)

Abstract: Renewable energy sources are connected to the grid through inverters, resulting in reduced grid inertia and poor stability. Traditional grid-connected inverters do not have the function of voltage and frequency regulation and can no longer adapt to the new development. The virtual synchronous generator (VSG) has the function of voltage and frequency regulation and has more outstanding advantages than the traditional inverter. Based on the principle of the VSG, the relationship between energy storage capacity, frequency response and output power of the VSG is derived, and the relationship between the virtual inertia coefficient, damping coefficient and frequency characteristics of the VSG and output power is revealed. The mathematical model is established and modeled using the Matlab/Simulink simulation software, and the simulation results verify the relationship between energy storage capacity and frequency response and the output power of the VSG.

Key words: damping coefficient, energy storage capacity, inertia coefficient, virtual synchronous machine

1. Introduction

With the rapid development of new energy sources, new energy sources represented by photovoltaic and wind power have been widely used [1–3]. However, due to the constraints of power output characteristics, new energy sources are generally grid-connected through power electronic interface devices. Therefore, this type of new energy is categorized as an inverter-based power supply [4, 5]. At present, these new energy sources are mainly grid-connected through inverters, which do not have the inertia and damping characteristics that generators have. The virtual synchronous generator (VSG) can simulate the inertia and damping inertia of synchronous generators, and it has been widely studied and applied once it was proposed [6, 7].

The VSG does not have a rotor, and mainly uses control algorithms to simulate the rotor generated rotational inertia and damping. The VSG achieves grid connection by simulating the actual output characteristics to achieve grid integration, which makes the stability of the grid consistent with that of conventional generators and facilitates the operation and management of the grid. The inertia and damping are mainly determined by the control algorithm of the inverter and the parameters of the energy storage device. There are more studies on the control algorithm and stability of the VSG, and less studies on the relationship between VSG parameters and energy storage device [8–10].

The literature [11] summarizes the principle models of various VSGs. The literature [12] proposes a power quality control strategy based on a small-signal virtual synchronizer microgrid. Reference [13] proposes a control strategy to improve the receiver-side converter of virtual synchronous machines. Reference [14] proposes a VSG frequency control strategy based on digital frequency protection to improve frequency stability and maintain dynamic safety of inertial systems. Reference [15] proposes an inertial fuzzy control that can dynamically adjust the inertia. References [16, 17] analyzed the effect of inertia and damping on the system performance by comparing the VSG control algorithm with the control algorithm of a conventional inverter. References [18–23] analyze the improved VSG control algorithm and its performance. Reference [24–26] analyze the strategy of virtual inertia distribution regulation for multi-VSG systems. The parameters of the VSG require not only the setting of the control algorithm, but also the support of the energy storage capacity, and most of the references mentioned above does not examine the influence of energy storage. Reference [7] investigates the methods of energy storage configuration in different settings to find the optimal energy storage configuration scheme, but does not account for the need of energy storage in terms of inertia and damping. Reference [27] investigated the energy storage model and the power control method for charging and discharging for PV applications of the VSG, but has not yet derived the capacity requirements of the VSG inertia and damping with respect to energy storage. Reference [28] investigated the optimal configuration structure of cells for energy storage systems, but has not yet calculated the inertia and damping of the VSG in relation to the capacity of the energy storage setup.

The capacity of the energy storage device has a very important influence on the design of the VSG. In this paper, we analyze the relationship between the energy storage capacity of the VSG and frequency response and output power, we also analyze the effect on frequency response and output power under different inertia and damping coefficients, as well as derive the corresponding relationship equation. The results can be used in the design of VSG parameters and the configuration of energy storage devices.

2. VSG mathematical modeling

Synchronous generators have rotors with a certain rotational inertia, so the system does not have a sudden change in frequency over a short period of time. The VSG, on the other hand, introduces virtual rotational inertia control in the control algorithm of the inverter to simulate the rotor inertia of the synchronous generator [29]. The mechanical rotation equation of the virtual synchronous generator is shown in Eq. (1).

$$J\frac{\mathrm{d}\omega}{\mathrm{d}t} = T_s - T_e - D(\omega - \omega_0), \tag{1}$$

where: T_s is the mechanical torque; T_e is the electromagnetic torque; D is the damping factor; J is the rotational inertia; ω is the actual rotor angular velocity; ω_0 is the rated rotor angular velocity.

Define the mechanical power as shown in Eq. (2).

$$P_s = T_s \cdot \omega_0 \,. \tag{2}$$

Define the electromagnetic power as shown in Eq. (3).

$$P_e = T_e \cdot \omega_0 \,. \tag{3}$$

From Eqs. (1)–(3), we can obtain Eq. (4).

$$J\frac{\mathrm{d}\omega}{\mathrm{d}t} = \frac{P_s}{\omega_0} - \frac{P_e}{\omega_0} - D(\omega - \omega_0). \tag{4}$$

The VSG simulates the rotor motion equation of the synchronous generator mainly by controlling the control algorithm of the inverter, (4). The rotational inertia and damping characteristics of the synchronous generator are simulated. The stability and sag characteristics of the VSG output voltage and frequency are achieved. The schematic diagram of the VSG is shown in Fig. 1.

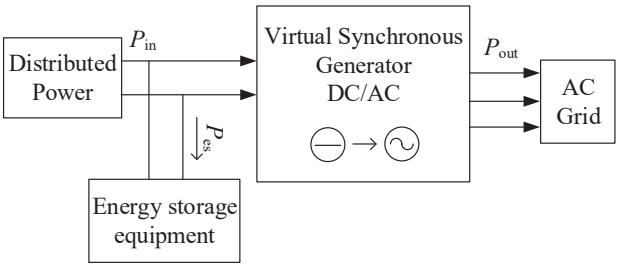

Fig. 1. Diagram of VSG system

In the figure: P_{out} is the output power; P_{in} is the input power; P_{es} is the charging and discharging power of the energy storage device; u_a, u_b, u_c are the three-phase voltages of the output; u_{ga}, u_{gb}, u_{gc} are the three-phase voltages of the grid; U_{dc} is the input DC bus voltage.

Consider that the angular frequency of the induced electric potential is the same as the rotor rotating mechanical angular frequency when the pole logarithm of the VSG is 1. From Eq. (4), Eq. (5) is obtained.

$$P_{\text{in}} - P_{\text{out}} = J\omega_0\frac{\mathrm{d}\omega}{\mathrm{d}t} + D\omega_0(\omega - \omega_0), \tag{5}$$

where: J is the rotational inertia of the VSG; D is the damping coefficient of the VSG.

Use P_{in0} to denote the rated input power of the VSG and P_{out0} to denote the rated output power of the VSG.

Let $\Delta\omega = \omega - \omega_0$, $\Delta P_{\text{in}} = P_{\text{in}} - P_{\text{in0}}$, and $\Delta P_{\text{out}} = P_{\text{out}} - P_{\text{out0}}$. Then $\Delta\omega$ denotes the difference between the output angular frequency and the rated angular frequency of the VSG. ΔP_{in} denotes the difference between the actual input power and the rated input power of the VSG. ΔP_{out} denotes

the difference between the actual output power and the rated output power of the VSG. Therefore, from Eq. (5), Eq. (6) is obtained as follows:

$$P_{\text{in0}} + \Delta P_{\text{in}} - P_{\text{out0}} - \Delta P_{\text{out0}} = J\omega_0 \frac{\mathrm{d}(\omega_0 + \Delta\omega)}{\mathrm{d}t} + D\omega_0\Delta\omega. \tag{6}$$

Equations (7) and (8) are obtained when the VSG is operated under rated steady-state operating conditions.

$$\omega = \omega_0\,, \tag{7}$$

$$P_{\text{in0}} = P_{\text{out0}}\,. \tag{8}$$

Equation (9) can be obtained from Eqs. (6)–(8).

$$\Delta P_{\text{in}} - \Delta P_{\text{out}} = J\omega_0 \frac{\mathrm{d}\Delta\omega}{\mathrm{d}t} + D\omega_0\Delta\omega. \tag{9}$$

The output active power of the generator can be expressed as Eq. (10).

$$P_{\text{out}} = 3\frac{UU_g}{\omega L}\sin\delta, \tag{10}$$

where: U denotes the u_a, u_b and u_c rms values; U_g denotes the u_{ga}, u_{gb} and u_{gc} rms values. Let $\Delta U = U - U_0$, $\Delta\delta = \delta - \delta_0$; U_0 denotes the rated values of u_a, u_b and u_c; δ_0 denotes the rated power angle of the VSG. Without considering the variation of the VSG output voltage and the grid voltage, Eq. (11) can be obtained as follows:

$$P_{\text{out0}} + \Delta P_{\text{out}} = 3\frac{UU_g}{\omega L}\sin(\delta_0 + \Delta\delta). \tag{11}$$

Since $\Delta\delta$ is small, then we have $\cos\Delta\delta \approx 1$, $\sin\Delta\delta \approx \Delta\delta$ and $\omega_0 + \Delta\omega \approx \omega_0$. Thus, Eq. (12) can be obtained as follows:

$$P_{\text{out0}} + \Delta P_{\text{out}} = 3\frac{UU_g}{\omega_0 L}\sin\delta_0 + 3\frac{UU_g}{\omega_0 L}\cos\delta_0\Delta\delta. \tag{12}$$

When U and U_g are constant, because $P_{\text{out0}} = 3\dfrac{U_0U_g}{\omega_0 L}\sin\delta_0$, Eq. (13) can be obtained.

$$\Delta P_{\text{out}} = 3\frac{U_0U_g}{\omega_0 L}\cos\delta_0\Delta\delta. \tag{13}$$

Let $K = 3\dfrac{U_0U_g}{\omega_0 L}\cos\delta_0$ be the synchronization factor of the VSG. Then Eq. (13) can be expressed as Eq. (14).

$$\Delta P_{\text{out}} = K\Delta\delta. \tag{14}$$

The amount of change of the VSG power angle can be expressed as Eq. (15).

$$\Delta\delta = \int_0^t (\Delta\omega - \Delta\omega_g)\,\mathrm{d}t, \tag{15}$$

where: $\Delta\omega_g = \omega_g - \omega_0$, ω_g is the grid frequency.

Equations (9), (14) and (15) represent the small-signal time-domain mathematical model of the VSG, and the Laplace transform is applied to it to obtain the small-signal frequency-domain mathematical model of the VSG, as shown in Eqs. (16)–(18).

$$\Delta P_{\text{in}} - \Delta P_{\text{out}} = J\omega_0 \Delta\omega s + D\omega_0 \Delta\omega, \tag{16}$$

$$\Delta P_{\text{out}} = K\Delta\delta, \tag{17}$$

$$\Delta\delta = \frac{\Delta\omega}{s}. \tag{18}$$

The block diagram of the transfer function of the VSG can be obtained according to Eqs. (16)–(18), as shown in Fig. 2.

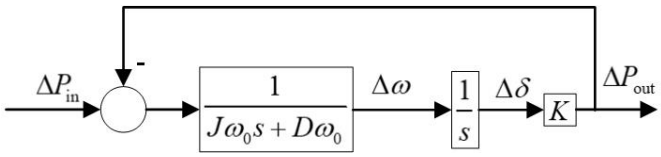

Fig. 2. Small signal model of VSG

Equation (19) can be obtained from Fig. 1.

$$P_{\text{in}} = P_{\text{out}} + \Delta P_{\text{es}} = P_{\text{in0}} + \Delta P_{\text{in}} = \Delta P_{\text{es}} + P_{\text{out0}} + \Delta P_{\text{out}}. \tag{19}$$

As a result, the charging and discharging power of the energy storage device can be obtained as in Eq. (20).

$$\Delta P_{\text{es}} = \Delta P_{\text{in}} - \Delta P_{\text{out}}. \tag{20}$$

The inertial response and FM response of the VSG are shown in Fig. 3. Throughout the frequency response, the rates of change amplitude, peak frequency, regulation time and steady-state frequency of the system appear sequentially in time order.

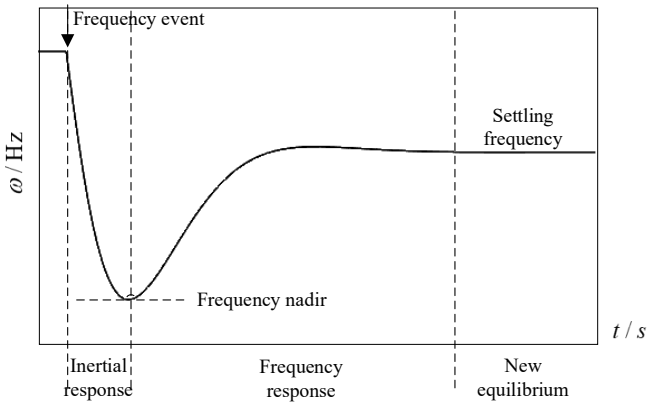

Fig. 3. Inertial response and frequency modulation response of VSG

3. Frequency response and output power of VSG as a function of energy storage capacity

The energy storage device is related to the inertia coefficient and damping coefficient of the VSG. The configuration of the VSG energy storage parameters is mainly based on the actual demand to determine the inertia coefficient and damping coefficient. Then the demand of energy storage is determined according to the parameters of the VSG and output power. The following is an analysis of the two main aspects of the frequency response and the relationship between output power and energy storage.

3.1. Relationship between VSG frequency response and energy storage capacity

The effects of input power disturbance and grid frequency variation are not considered. Based on Fig. 2, the relationship between the frequency response and energy storage capacity is shown in Eq. (21).

$$\frac{\Delta\omega}{\Delta P_{\text{es}}} = \frac{1}{J\omega_0 s + D\omega_0} \,. \tag{21}$$

Equation (21) indicates that the system can adjust the VSG power angle by adjusting the frequency ω for a first-order system.

The time constant T is shown in Eq. (22).

$$T = \frac{J}{D} \,. \tag{22}$$

The inverse Laplace transform of the step response of the transfer function of Eq. (21) yields Eq. (23).

$$\Delta\omega = \Delta P_{\text{es}} \frac{1 - e^{-\frac{D}{J}t}}{D\omega_0} \,. \tag{23}$$

The derivative of Eq. (23) shows that the function is monotonic and takes extreme values at the t infinity. The maximum value of $\Delta\omega$ can be obtained as shown in Eq. (24).

$$\Delta\omega_{\text{max}} = \Delta P_{\text{es}} \frac{1}{D\omega_0} \,. \tag{24}$$

From Eq. (24), we can see that the larger the damping factor D, the smaller the frequency variation of the VSG and the better the stability.

3.2. Relationship between VSG output power and energy storage capacity

The relationship between the output power and energy storage capacity is shown in Eq. (25).

$$\frac{\Delta P_{\text{out}}}{\Delta P_{\text{es}}} = \frac{K}{J\omega_0 s^2 + D\omega_0 s} \,. \tag{25}$$

Equation (25) is a second-order system. The angular frequency of the oscillation ω_n and the damping ratio ζ of this transfer function are shown in Eq. (26).

$$\begin{cases} \omega_n = \sqrt{\dfrac{K}{J\omega_0}} \\ \zeta = \dfrac{D}{2}\sqrt{\dfrac{\omega_0}{JK}} \end{cases}. \tag{26}$$

The inverse Laplace transform of the step response of the transfer function of Eq. (25) yields Eq. (27).

$$\Delta P_{\text{out}} = \Delta P_{\text{es}} \frac{JK}{D^2\omega_0}\left(\frac{D}{J}t - 1 + e^{-\frac{D}{J}t}\right). \tag{27}$$

From Eq. (27), it can be seen that when the input power is constant, the energy storage capacity is larger. The more power can be output, the larger the energy storage capacity can ensure the stability of the output power.

4. Simulation analysis

To verify the relationship between the charging and discharging power and capacity parameters of the energy storage device, the inertia coefficient and damping coefficient of the VSG are studied. A model is built in Matlab/Simulink for simulation. The relevant parameter settings are shown in Table 1.

Table 1. Parameters of VSG

Parameter name	Unit	Value
J	kg·m^2	56.3
D	N·m·s	2073.9
K	W·rad^{-1}	6×10^6
ω_0	rad·s^{-1}	100π
U_0	kV	6.6

For VSG simulation, ΔP_{es} is set to 1 MW.

4.1. Verification of the relationship between VSG frequency response and energy storage capacity

The simulation curve of the frequency response versus energy storage capacity is shown in Fig. 4.

The simulation results in Fig. 4 verify Eq. (24).

The VSG selected the parameters shown in Table 1, changed J and D, and simulated the frequency response. The results are shown in Fig. 5.

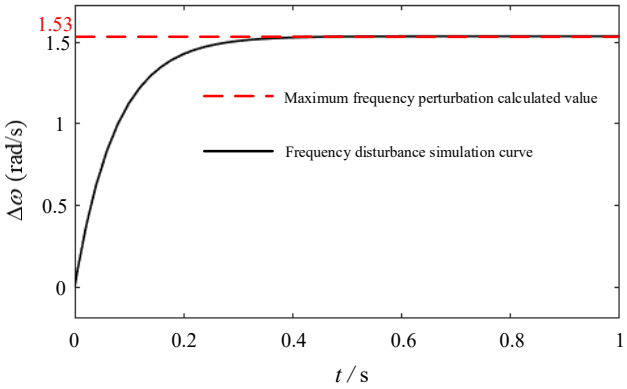

Fig. 4. Simulation diagram of frequency characteristics of VSG

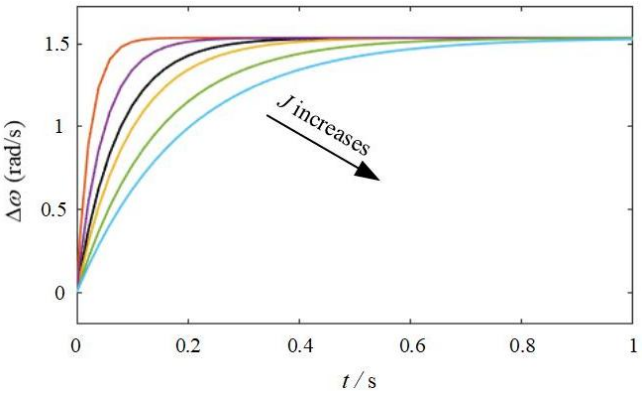

(a) J changes

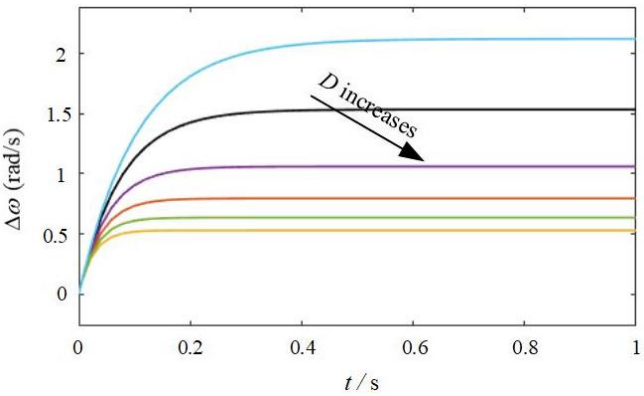

(b) D changes

Fig. 5. Effect of VSG parameters on frequency characteristics

As can be seen from Fig. 5, the smaller the inertia coefficient J is, the shorter the time required for frequency tuning. However, the smaller the inertia coefficient J is, the greater the rate of change of the initial frequency adjustment. If high-frequency interference occurs in the input power, the inertia coefficient is too small, which will lead to violent oscillation of the VSG frequency and the performance becomes poor. Therefore, in order to enhance the anti-interference capability, the inertia coefficient should not be too small. The larger the damping factor D, the shorter the frequency adjustment time, the better the anti-interference performance of the VSG.

The VSG selects the parameters in Table 1 and varies ΔP_{es}. The frequency response is simulated and the results are shown in Fig. 6.

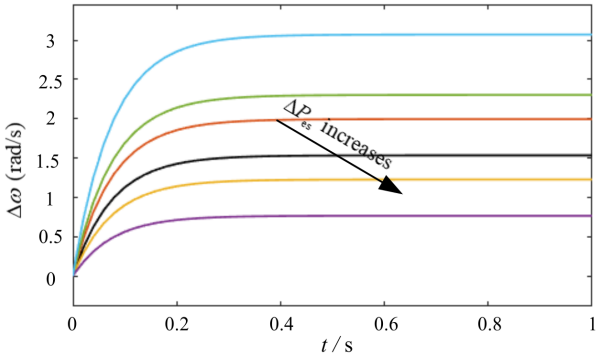

Fig. 6. Simulation of frequency response under different energy storage capacity

As can be seen from Fig. 6, when the stored energy becomes larger, the frequency response takes longer to reach stability, and the time required for frequency stabilization is longer when the stored energy capacity is larger.

4.2. Verification of the relationship between VSG output power and energy storage capacity

The simulation curve of the VSG output power versus the energy storage capacity using the parameters in Table 1 is shown in Fig. 7.

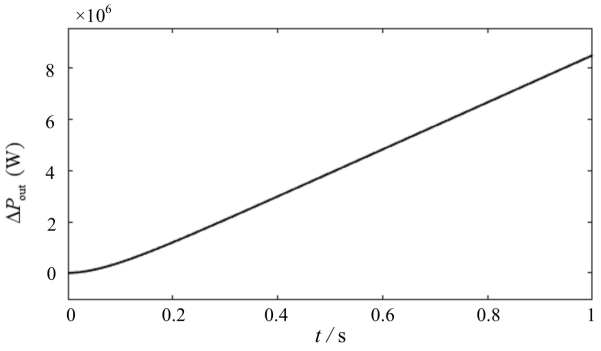

Fig. 7. Simulation of VSG output power and energy storage device capacity

Equation (27) verifies the value of the simulation results in Fig. 7.

The VSG selects the parameters in Table 1 and varies J and D. The output power is simulated and the results are shown in Fig. 8.

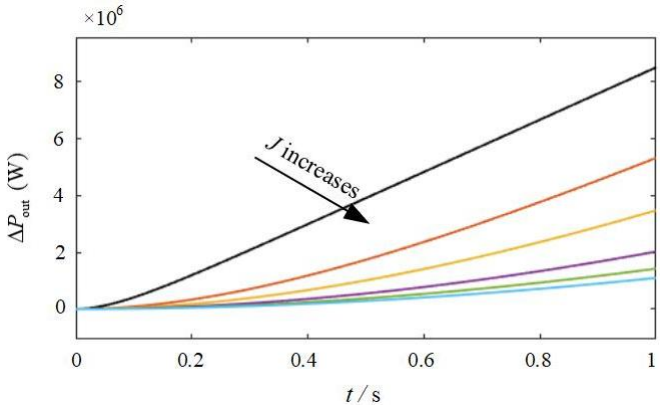

(a) J changes

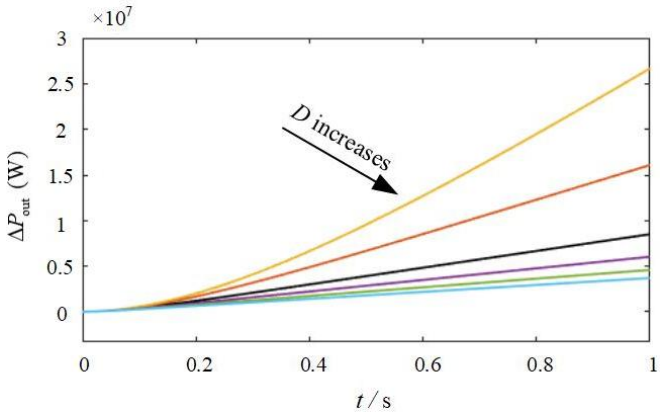

(b) D changes

Fig. 8. Effect of VSG parameters on output power

As can be seen from Fig. 8, the larger the inertia coefficient J, the smaller the power output in the same time. The larger the inertia coefficient J, the greater the power output. The larger the damping coefficient D, the smaller the power output in the same time. The smaller the damping factor D, the greater the power output in the same time. Therefore, if you want to increase the output power, you can adjust the inertia coefficient and damping coefficient. If you want to reduce the output power, you can adjust the inertia coefficient and damping coefficient.

The VSG selects the parameters in Table 1 and varies the ΔP_{es}. The output power is simulated and the results are shown in Fig. 9.

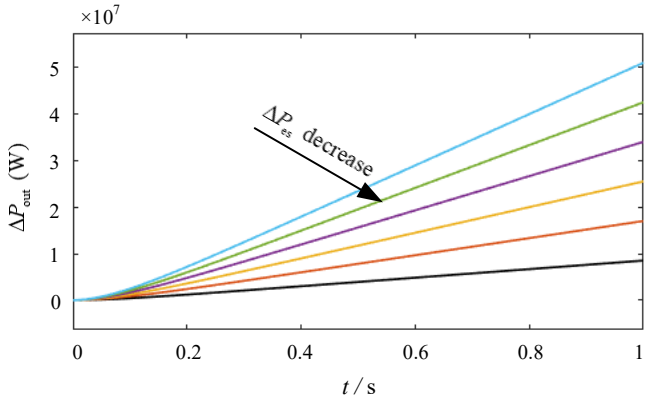

Fig. 9. Simulation of output power under different energy storage capacity

As can be seen from Fig. 9, when the ΔP_{es} decreases, the corresponding output power decreases. If the stability of the output power is to be improved, the energy storage capacity needs to be increased.

5. Conclusion

In this paper, the relationship between the frequency characteristics, output power and energy storage capacity of the VSG is derived in detail. The simulation was verified by Matlab/Simulink. The results of the study show that:

1. In order to improve the anti-interference capability of VSG output power, the inertia coefficient needs to be increased; to reduce the range of VSG frequency variation due to grid frequency change, the damping coefficient needs to be increased. A larger capacity of energy storage equipment is also required.
2. When the energy storage capacity of the VSG is insufficient, it will not be possible to control the output of the VSG as expected and will cause voltage fluctuations. Therefore, the actual design should meet the minimum charging and discharging requirements of the VSG.
3. When the inertia coefficient and damping coefficient are smaller, the output power will be larger, and it will meet the high-power output.
4. The VSG has the same output characteristics as a conventional synchronous generator, justifying the establishment of a model that facilitates more efficient use of new energy sources.

References

[1] Yan X.W., Zhang W.C., *Review of VSG control-enabled universal compatibility architecture for future power systems with high-penetration renewable generation*, Applied Sciences, vol. 9, no. 7, p. 1484 (2019), DOI: 10.3390/app9071484.

[2] Lopes J.A.P., Hatziargyriou N., Mutale J., *Integrating distributed generation into electric power systems: a review of drivers, challenges and opportunities*, Electric Power Systems Research, vol. 77, no. 9, pp. 1189–1203 (2007), DOI: 10.1016/j.epsr.2006.08.016.

[3] Yan X.W., Xu Y., *Multiple time and space scale reactive power optimization for distribution network with multi-heterogeneous RDG participating in regulation and considering network dynamic reconfiguration*, Transactions of China Electrotechnical Society, vol. 34, no. 20, pp. 4358–4372 (2019), DOI: 10.19595/j.cnki.1000-6753.tces.181933.

[4] Zhang W.C., Liang H.F., Bin Z., *Review of DC technology in future smart distribution grid*, IEEE PES Innovative Smart Grid Technologies, Tianjin, China, pp. 1–4 (2012).

[5] Guarnieri M., *More light on information*, IEEE Industrial Electronics Magazine, vol. 9, no. 4, pp. 58–61 (2015), DOI: 10.1109/MIE.2015.2485182.

[6] Zhang C.Y., Dou X.B., Sheng W.X., *A robust virtual synchronization control strategy for distributed photovoltaic clusters*, Proceedings of the CSEE, vol. 40, no. 2, pp. 510–521 (2020), DOI: 10.13334/j.0258-8013.pcsee.182424.

[7] Albu M., Visscher K., Creanga D., *Storage selection for DG applications containing virtual synchronous generators*, IEEE Bucharest Power Tech., Bucharest, Romania, pp. 1–6 (2009).

[8] Falahi G., Huang A., *Low voltage ride through control of modular multilevel converter based HVDC systems*, IECON 2014-40th Annual Conference of the IEEE Industrial Electronics Society, Dallas, TX, USA, pp. 4663–4668 (2014).

[9] Moulichon V., Debusschere V., Garbuio L., Rahmani M.A., Alamir M., Hadjsaid N., *Standardization tests for the industrialization of grid-friendly Virtual Synchronous Generators*, Archives of Electrical Engineering, vol. 68, no. 4, pp. 679–688 (2020), DOI: 10.24425/bpasts.2020.134181.

[10] Zhong Q.C., *Power-electronics-enabled autonomous power systems: architecture and technical routes*, IEEE Transactions on Industrial Electronics, vol. 64, no. 7, pp. 5907–5918 (2017), DOI: 10.1109/TIE.2017.2677339.

[11] Tan S., Geng H., Yang G., *Modeling framework of voltage-source converters based on equivalence with synchronous generator*, Modern Power Systems, vol. 6, no. 6, pp. 1291–1305 (2018), DOI: 10.1007/s40565-018-0433-1.

[12] Zhang B.Q., Hu C.B., Ma F.L., *Active Power Quality Control for Microgrid with Virtual Synchronous Generator Based on Small-signal Stability Analysis*, Automation of Electric Power Systems, vol. 43, no. 23, pp. 210–222 (2019), DOI: 10.7500/AEPS20190118001.

[13] Chen J.K., Zeng Q., Xin Y.C., *Secondary Frequency Regulation Control Strategy of MMC-MTDC Converter Based on Improved VSG*, Power System Technology, vol. 44, no. 4, pp. 1428–1436 (2020), DOI: 10.13335/j.1000-3673.pst.2019.1227.

[14] Daili Y., Harrag A., *New model of multi-parallel distributed generator units based on virtual synchronous generator control strategy*, Energy, Ecology and Environment, vol. 4, no. 5, pp. 222–232 (2019), DOI: 10.1007/s40974-019-00128-3.

[15] Gaber Magdy, Shabib G., Elbaset Adel A., *Renewable power systems dynamic security using a new coordination of frequency control strategy based on virtual synchronous generator and digital frequency protection*, International Journal of Electrical Power and Energy Systems, vol. 109, pp. 351–368 (2019), DOI: 10.1016/j.ijepes.2019.02.007.

[16] Liu J., Miura Y., Ise T., *Comparison of dynamic characteristics between virtual synchronous generator and droop control in inverter-based distributed generators*, IEEE Transactions on Power Electronics, vol. 31, no. 5, pp. 3600–3611 (2016), DOI: 10.1109/TPEL.2015.2465852.

[17] Luo A., Dong Y.T., Zhou X.P., *Sequence-impedance-based stability comparison between vsgs and traditional grid-connected inverters*, IEEE Transactions on Power Electronics, vol. 34, no. 1, pp. 46–52 (2019), DOI: 10.1109/TPEL.2018.2841371.

[18] Lu F.Z., He A.R., Hou K., *Low-voltage ride-through control strategy of virtual synchronous generator based on all-pass filter*, Electric Power Automation Equipment, vol. 39, no. 5, pp. 176–181 (2019), DOI: 10.16081/j.issn.1006-6047.2019.05.026.

[19] Aliipoor J., Miura Y., Ise T., *Power system stabilization using virtual synchronous generator with alternating moment of inertia*, IEEE Journal of Emerging and Selected Topics in Power Electronics, vol. 3, no. 2, pp. 451–458 (2015), DOI: 10.1109/JESTPE.2014.2362530.

[20] Li D., Zhu Q., Lin S., *A self-adaptive inertia and damping combination control of VSG to support frequency stability*, IEEE Transactions on Energy Conversion, vol. 32, no. 1, pp. 397–398 (2017), DOI: 10.1109/TEC.2016.2623982.

[21] Li X., Chen G., Ali M. S., *Improved virtual synchronous generator with transient damping link and its seamless transfer control for cascaded H-bridge multilevel converter-based energy storage system*, IET Electric Power Applications, vol. 13, no. 10, pp. 1535–1543 (2019), DOI: 10.1049/iet-epa.2018.5722.

[22] Hong H.H., Gu W., Huang Q., *Power Oscillation damping control for microgrid with multiple VSG units*, Proceedings of the CSEE, vol. 39, no. 21, pp. 6247–6254 (2019), DOI: 10.13334/j.0258-8013.pcsee.181088.

[23] Zeng Z., Shao W.H., Ran L., *Mathematical model and strategic energy storage selection of virtual synchronous generators*, Automation of Electric Power Systems, vol. 39, no. 13, pp. 22–31 (2015), DOI: 10.7500/AEPS20140901007.

[24] Song Q., Zhang H., Sun K., *Improved adaptive control of inertia for virtual synchronous generators in islanding micro-grid with multiple distributed generation units*, Proceedings of the CSEE, vol. 37, no. 2, pp. 412–423 (2017), DOI: 10.13334/j.0258-8013.pcsee.161658.

[25] Shi R., Zhang X., Hu C., *Self-tuning virtual synchronous generator control for improving frequency stability in autonomous photovoltaic-diesel micro grids*, Journal of Modern Power Systems and Clean Energy, vol. 6, no. 3, pp. 482–494 (2018), DOI: 10.1007/s40565-017-0347-3.

[26] Yang F., Shao Y.L., Li D.D., *A fuzzy adaptive VSG control strategy considering energy storage capacity and constraint of SOC*, Power System Technology, to be published.

[27] Prakash Ayyappan B., Kanimozhi R., *Design and analysis of the performance of multi-source interconnected electrical power system using resilience random variance reduction technique*, Archives of Electrical Engineering, vol. 69, no. 5, pp. 679–688 (2021), DOI: 10.24425/bpasts.2021.137941.

[28] Gao J.R., Li G.J., Wang K.Y., *Control of grid-connected PV-battery virtual synchronous machine considering battery charging/discharging power limit*, Automation of Electric Power Systems, vol. 44, no. 4, pp. 134–141 (2020), DOI: 10.7500/AEPS20190515010.

[29] Xing D.F., Tian M.X., *Relationship between frequency characteristics of virtual synchronous generator and parameters of energy storage equipment*, Power system technology, vol. 45, no. 9, pp. 3582–3593 (2021), DOI: 10.13335/j.1000-3673.pst.2020.1490.